Sādhanā Vol. 28, Parts 1 & 2, February/April 2003, pp. 263–272. © Printed in India

Superconductivity in MgB_2: Phonon modes and influence of carbon doping

A BHARATHI, Y HARIHARAN, JEMIMA BALASELVI and C S SUNDAR

Materials Science Division, Indira Gandhi Centre for Atomic Research, Kalpakkam 603 102, India
e-mail: css@igcar.ernet.in

Abstract. Following a brief overview, results of our investigations on phonon modes in MgB_2, and superconducting transition in carbon doped MgB_2 are presented. The superconducting transition temperature in $MgB_{2-x}C_x$ as obtained from susceptibility and resistivity measurements is observed to decrease systematically from 39·4 K for $x = 0$ to 26 K for $x = 0{\cdot}5$. It is shown the changes in lattice volume, as obtained from x-ray diffraction measurements, can account only partially for the observed decrease in T_c. The observed variation of T_c with carbon content is seen to correlate with the Debye temperatures, obtained from an analysis of the resistivity data.

Investigation of the phonon modes in MgB_2, through infrared absorption measurements indicate three modes at 410, 475 and 560 cm^{-1}. The former two are associated with the infrared active modes, and the third component is associated with the Raman mode, that gets activated due to disorder. A study of the temperature dependence of these modes indicates no changes across the superconducting transition. The mode at 560 cm^{-1} shows a significant hardening and a corresponding decrease in linewidth, with the lowering of temperature, that can been accounted in terms of anharmonicity.

Keywords. Superconductivity; MgB_2; carbon-doping; susceptibility; resistivity; infrared spectroscopy.

1. Introduction and overview

The serendipitous discovery of superconductivity at 39K in the binary intermetallic MgB_2 by Nagamutsu *et al* (2001) has initiated a flurry of activity. In a short period of time extensive studies (for a review, see Buzea & Yamashita 2000) have been carried out on the normal state and superconducting properties, which include the determination of the superconducting gap, coherence length, penetration depth and critical fields. Theoretical calculations (An & Pickett 2001; Kong *et al* 2001; Kortus *et al* 2001) indicate that superconductivity in this system can be understood in the framework of electron–phonon interaction. Initial evidence for the importance of electron–phonon interaction was provided by the experiments on boron isotope effect (Bud'ko *et al* 2001) MgB_2 has been syntheised in a variety of forms such as thin films

(Kang *et al* 2001), tapes and wires (Canfield *et al* 2001), and large critical current densities $\sim 10^6$ A /cm^2 have been obtained (Kang *et al* 2001) in thin films. This together with the transparency of grain boundaries, an aspect that has plagued the cuprate superconductors, point to the considerable prospect for large scale applications and devices (Buzea & Yamshita 2002).

MgB_2 crystallises in the hexagonal structure, consisting of alternating honeycomb layers of B and closed packed layers of Mg. Electronic structure calculations (An & Pickett 2001; Kong *et al* 2001; Kortus *et al* 2001) indicate that in this system Mg is completely ionized, and the bands at the Fermi level are derived from the σ orbitals of boron. The hole- carriers in the metallic B layer has been shown to have considerable electron–phonon interaction with the optically active vibrational modes. MgB_2 has four distinct optic modes: two of which involve the displacement of B with respect to Mg, which are IR active, the in-plane displacement of B, that is Raman active, and a silent mode involving displacement of B along the z direction. Of all these optic modes, the Raman active mode has been shown to have dominant coupling with the σ orbitals of boron (An & Pickett 2001; Kong *et al* 2001). The Raman active mode has also been shown to be highly anharmonic (Yildrim *et al* 2001). Given the importance of the Raman mode, there have been several (Chen *et al* 2001; Martinho *et al*; Goncharev *et al* 2001; Bohnen & Renker 2001; Hlinka *et al* 2001) Raman scattering experiments on MgB_2, which include studies on the electronic background (Chen *et al* 2001), experiments on the variation of Raman mode as a function of temperature (Martinho *et al*), and pressure (Goncharev *et al* 2001). Infrared spectroscopy has been used (Tu *et al*) to determine the superconducting gap in MgB_2.

As with the discovery of any new superconducting system, several studies have been made on doped MgB_2, with most detailed measurements on Al doped (Slusky *et al* 2001) MgB_2. These doping studies are important for it may lead to a new system with increased T_c, or the dopants may act as pinning centre to increase the critical current density. While several substitutions have been tried in MgB_2, in all cases T_c has been observed to decrease, with the exception of Zn (Moritomo & Xu; Khazakov *et al*) and Nb (Kalavathi *et al* 2001) in which a slight increase has been reported. We may also add that doping studies also help to discriminate between various models and thus contribute to the understanding of the mechanism of superconductivity.

In this paper, we focus on two of our recent investigations on MgB_2: studies on superconductivity in carbon doped MgB_2 (Jemima Balaselvi *et al* 2001), and investigations of the temperature dependence of vibrational modes in MgB_2 through infrared spectroscopy (Sundar *et al* 2001).

2. Sample preparation

Our investigations are on bulk polycrystalline samples, prepared by solid state reaction of fine powder of Mg and B. One of the crucial issues in the synthesis of stoichiometric MgB_2 is related to the volatility of Mg and the fact that Mg is highly reactive. This necessitates sealing the starting materials in Ta tubes under Ar atmosphere, to prevent the attack of quartz tubes used for heat treatment under vacuum. During the course of these investigations, we have evolved an elegant method of sealing the initial mixture under a high pressure of Ar and carrying out the heat treatment. Stoichiometric quantities of Mg (99·9%), amorphous boron (99%), were ground and pelletised, and loaded into a Ta crucible which was subsequently placed into a thick walled SS tube closed at the bottom. After a few initial evacuations and Ar flushings, the SS tube is filled with high purity Ar gas at a pressure of 35 bar. With the help of a needle valve this pressure is locked inside the tube. The SS tube assembly is fitted via a Wilson seal to an outer quartz tube, which is evacuated to 10^{-5}torr. The entire assembly

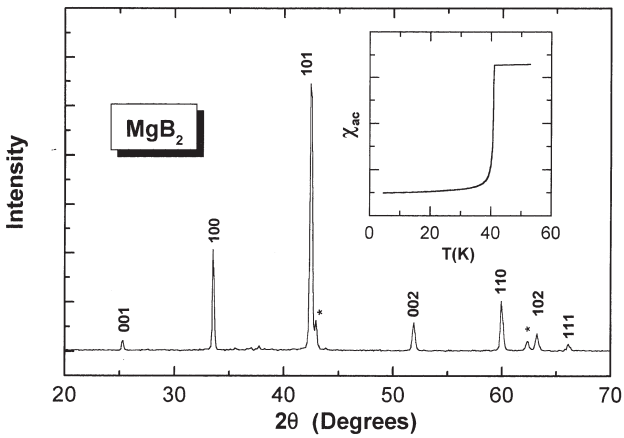

Figure 1. X-ray diffraction pattern of MgB_2 indexed to hexagonal $P6/mmm$ structure. The impurity lines due to MgO are indicated by asterisks. The inset shows the superconducting transition at 39·4 K.

of quartz tube and SS tube containing the sample is inserted into a vertical furnace kept at 900°C. The heat treatment is carried out for 1 h and 30 min, during which the Ar pressure is seen to rise to 50 bar. After the heat treatment the furnace is switched off, and the cold sample is removed from the SS tube and weighed. No Ar gas leak was observed during this heat treatment. The weight loss of the sample after the heat treatment was negligible, recorded to be routinely $< 1\%$.

Figure 1 shows the X-ray diffraction pattern of MgB_2 obtained from the heat treatment under 50 bar of Ar. It can be seen that all the peaks can be indexed to the hexagonal *(P6/mmm)* structure with lattice parameters $a = 3{\cdot}0846$ Å and $c = 3{\cdot}5224$ Å, which are in good agreement with the reported values (Nagamutsu *et al* 2001). A small amount $\sim 1\%$ of MgO is obtained as an impurity phase. No signature of unreacted B is seen in the XRD measurements. The superconducting transition, as measured through ac susceptibility technique, is shown in the inset. The superconducting fraction is estimated to be $\sim 75\%$.

3. Superconductivity in carbon doped MgB_2

Given that superconductivity in MgB_2 arises due to hole carriers on the B layer interacting with the high frequency in-plane B vibrations, there have been theoretical calculations (Mehl *et al*) that predict the possibility of an increase in T_c by chemical substitution on the Mg sublattice by a monovalent cation, viz. Cu, to increase the hole concentration, along with a C substitution in the B sublattice to increase the stiffness of the boron layer. Following this clue, we have carried out detailed investigation on the influence of carbon on superconductivity in MgB_2, through *ac* susceptibility and resitivity measurements, coupled with structure determination through X-ray diffraction. Earlier studies (Moritomo & Xu; Nagamutsu *et al* 2001) on C substitution have been inconclusive: While Takenobu *et al* show that T_c decreases with C substitution up to the solubility limit of $x = 0{\cdot}10$, beyond which superconductivity disappears, Paranthaman *et al* (2001) claim that T_c remains unchanged with C substitution, and that the volume fraction of the superconducting phase decreases with carbon substitution due to its precipitation at the grain boundaries. We therefore examine in detail the influence of C doping on the superconductivity of MgB_2.

Figure 2 shows the results of *ac* susceptibility measurements (Jemima Balaselvi *et al* 2001) on C doped MgB_2. In undoped MgB_2, a sharp superconducting transition is observed at

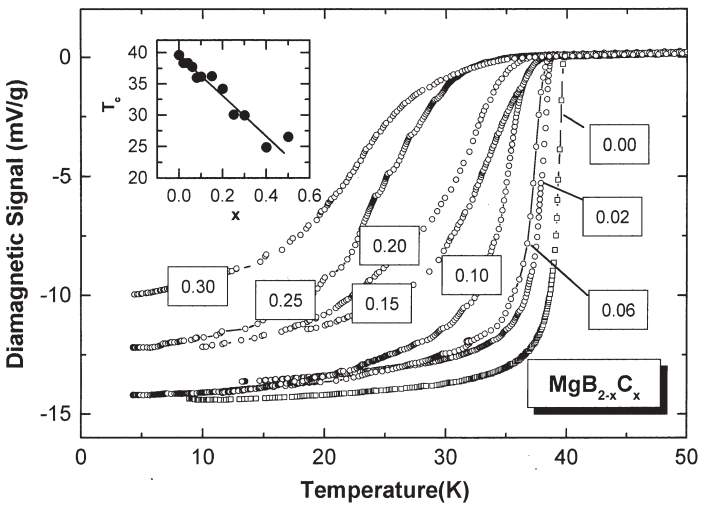

Figure 2. Susceptibilty measurements indicating the superconducting transition in $MgB_{2-x}C_x$. The inset shows the variation of T_c with carbon content x.

39·4 K. With the increase of C content, the superconducting transition is seen to decrease and the resulting transition temperatures are shown in the inset. While the magnitude of the diamagnetic signal at lowest temperature measured, decreases with the increase of carbon concentration, bulk superconductivity persists even for carbon substitutions of $x = 0{\cdot}3$.

To obtain further insight into the observed decrease of T_c with carbon content, we have carried out (Jemima Balaselvi *et al* 2001, 2002) structural investigations using X-ray diffraction on various C doped samples, and resistivity measurements as a function of temperature. X-ray diffraction measurements indicate that in $MgB_{2-x}C_x$, the hexagonal structure is retained up to $x = 0{\cdot}25$. Analysis of these diffraction patterns show a substantial decrease in the a-axis parameter (see figure 3) and a small but systematic increase in the c-axis lattice parameter with increase in C fraction. The resulting change in the unit cell volume is shown in the inset. We note that we observe single phase samples up to $x = 0{\cdot}25$, and do not see evidence for phase separation beyond $x = 0{\cdot}08$ (Takenobu *et al*).

Temperature-dependence of resistivity in $MgB_{2-x}C_x$ was carried out in standard four-probe geometry and results are shown in figure 4. In undoped MgB_2, the resitivity in the normal state shows a clear metallic behaviour, with a sharp resistive transition to the superconducting state at 39·4 K. This together with the large value of residual resistivity ratio points to the good quality of the sample. The resistivity in the normal state is seen to increase with carbon content. The temperature dependence of resistivity in the normal state as shown in figure 4, arises due to scattering of electrons by phonons. We have analysed (Jemima Balaselvi *et al* 2002) these data for each of the carbon doped samples using the Bloch–Gruneissen formalism, from which the Debye temperature, θ_D has been estimated. The resulting variation of θ_D with carbon content is shown in the inset.

The T_c variation with carbon content, as obtained from susceptibility and resitivity measurements, is shown in figure 5. Within the framework of BCS theory, such a decrease in T_c could arise due to (Jemima Balaselvi *et al* 2002) the decrease in the characteristic phonon frequency, θ_D, and/or the changes in the electron density of states at the Fermi level, $N(E_F)$. We note from the inset of figure 3, that the lattice volume decreases with carbon content. This could lead to a broadening of the electron density of states and a consequent lowering of $N(E_F)$. Earlier experiments on the variation of T_c with pressure (Lorenz *et al* 2001) indi-

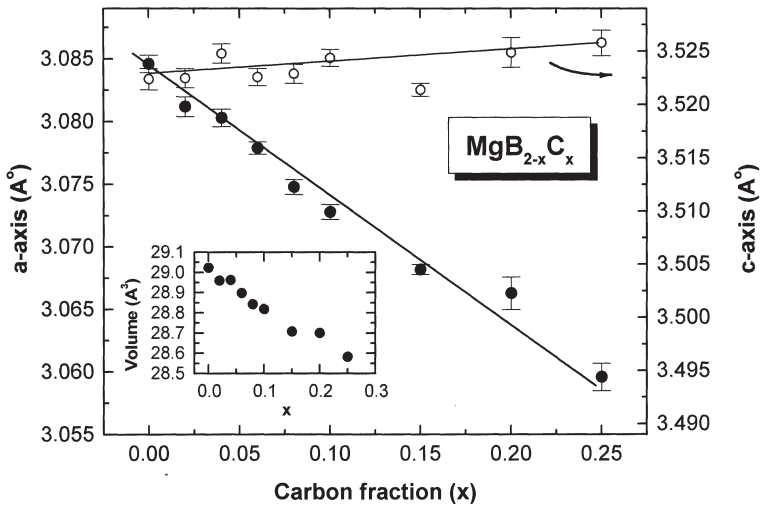

Figure 3. Variation of lattice parameters with carbon content in $MgB_{2-x}C_x$. The inset shows the variation of lattice volume with carbon concentration.

cate a decrease in the superconducting transition temperature at the rate of 1K/GPa. Using the measured (Bordet *et al*) bulk modulus of MgB_2, this translates to a reduction of T_c with volume at the rate of $5{\cdot}6\,\mathrm{K/A}^3$. Thus, from the experimentally measured changes in lattice parameter (see figure 3) with C content, the expected decrease in T_c due to the change in the lattice volume can be estimated, and this is indicated by the dashed line in figure 6. It is seen that the volume decrease obtained on carbon doping, by itself, cannot account for the observed decrease in T_c. However, we note that T_c decreases linearly from 39 to 26 K, when the carbon content increases to $x = 0{\cdot}5$, and the fractional change in T_c is similar to that in θ_D (see figures 5 and 6). This suggests that the decrease in T_c with carbon doping arises largely

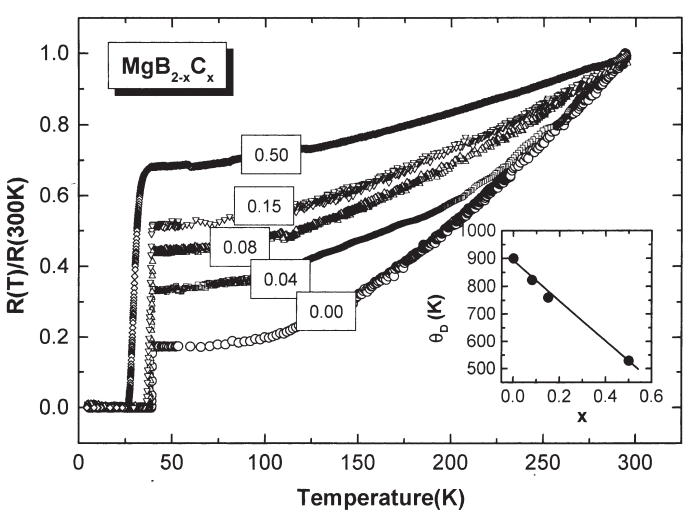

Figure 4. Superconducting transition in $MgB_{2-x}C_x$ as seen in resitivity measurements. The resistivity in the normal state has been fitted to Bloch–Gruneissen expression. The inset shows the variation of Debye temperature, θ_D with carbon content.

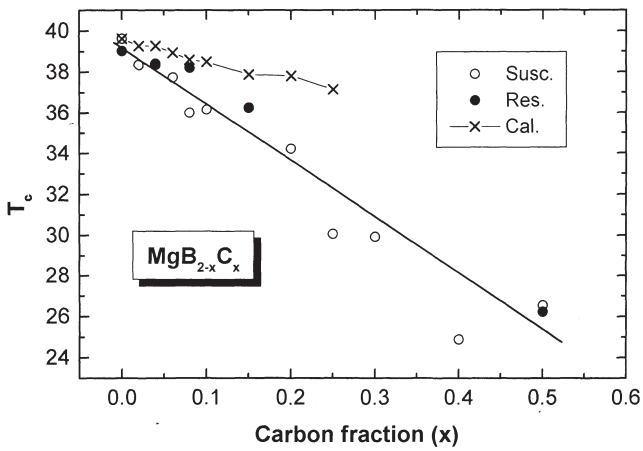

Figure 5. Variation of T_c with carbon content in $MgB_{2-x}C_x$, as obtained from susceptibility and resistivity measurements. The dashed line indicates the expected decrease in T_c due to volume change (see text).

due to the decrease in θ_D with the increase of C content in $MgB_{2-x}C_x$ (Jemima Balaselvi *et al* 2002).

Further experimental evidence for the reduction of Debye temperature with carbon doping, such as from specific heat measurements or vibrational spectroscopy, will be useful, as also calculations on the electronic structure to look for the changes in the electron density of states induced by carbon doping of MgB_2.

4. Phonon modes in MgB_2

As indicated in the introduction, there is a widespread consensus that superconductivity in MgB_2 can be rationalized within the framework of electron–phonon interaction (An & Pickett

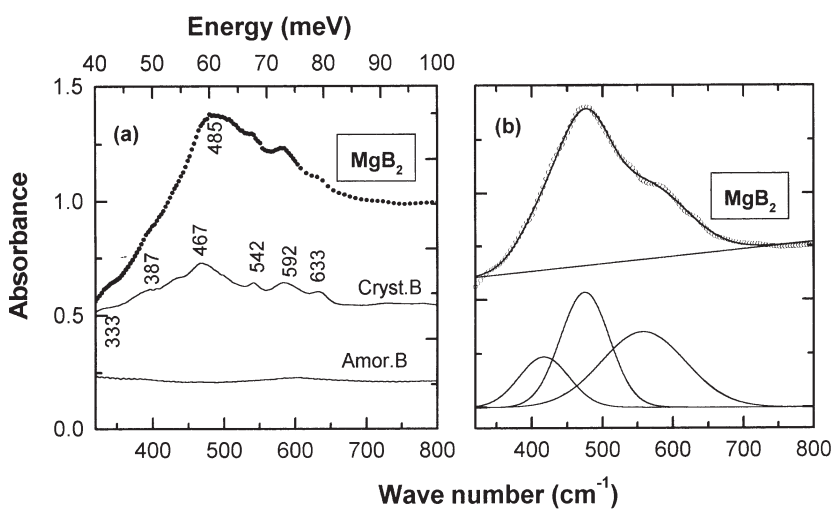

Figure 6. **(a)** Absorption spectrum of MgB_2. Also shown are the absorption spectra of the starting crystalline and amorphous B. **(b)** Fits of the absorption spectrum at 297 K in terms of sum of three Gaussians and a linear background.

2001; Kong *et al* 2001; Kortus *et al* 2001). Of particular importance is the Raman mode, involving the in-plane displacement of boron atoms, that couples strongly to the hole carriers in the B layer. Experimental studies (Bohnen & Renker *et al* 2001) show that the Raman mode centred at $\sim 580\,\mathrm{cm}^{-1}$ is characterized by a large linewidth ($\sim 200\,\mathrm{cm}^{-1}$) indicative of strong electron–phonon interaction. Studies on the temperature dependence (Martinho *et al*) of this mode point to the large anharmonicity of this vibrational mode. In the present study (Sundar *et al* 2001), we focus on the infrared spectroscopic studies of the phonon modes in MgB_2 – in particular the temperature variation of phonon modes across T_c.

Infrared absorption measurements were carried out on finely ground MgB_2 sample pelletized along with KBr, using a BOMEM-DA8 spectrometer, operating with a resolution of $4\,\mathrm{cm}^{-1}$. The temperature variation (300 to 5 K) was achieved using a JANIS continuous flow cryostat. Figure 6a shows the IR absorbance of MgB_2 in the range of 300 to $800\,\mathrm{cm}^{-1}$, the range in which the optic modes are predicted to exist. The absorption spectrum is characterised by a broad maximum at $485\,\mathrm{cm}^{-1}$, with small features at 333, 387, 542, 592 and $634\,\mathrm{cm}^{-1}$. These latter features can be associated with small amount of unreacted B, as can be seen from a comparison with the spectrum of crystalline B, that is also shown. The presence of unreacted B however, is not reflected in the XRD pattern (see figure 1), probably due to their small scattering power.

We note that the absorption spectrum in figure 6a bears a strong resemblance to the phonon density of states in the region of optical modes, as measured in the neutron scattering experiments (Osborne *et al* 2001; Yildrim 2001). In the light of theoretical calculations (An & Pickett 2001; Kong *et al* 2001; Kortus *et al* 2001; Yildrim 2001), which indicate the presence of two IR modes and a Raman mode in this spectral range, we analyse our spectrum in terms of three Gaussian components with a linear background as shown in figure 6b. In this analysis, we have disregarded the small blips, which as we have indicated earlier arise due to the second phase of B. The resulting components are observed at 410, 475 and $560\,\mathrm{cm}^{-1}$. The two low energy modes can be identified with IR active modes, and the third component at $560\,\mathrm{cm}^{-1}$, having a larger width of $140\,\mathrm{cm}^{-1}$, is identified with the Raman mode that gets activated due to disorder. In the IR reflectivity measurements by Tu *et al*, phonon features are seen at 380, 480 and 510 cm^{-1}, the former two identified with the IR modes and the latter with the Raman mode.

4.1 *Temperature dependence mode frequencies and widths*

In figure 7 we summarise the results on the temperature variation of the line position and widths of the three modes indicated in figure 6. With the lowering of temperature no significant variation of the mode frequency of the IR modes is observed. However, in the case of Raman mode, there is a significant hardening of mode frequency, associated with a reduction in the linewidth. This is reminiscent of anharmonicty effects. Within the framework of the cubic anharmonicty model (Sood *et al* 1981), the temperature dependence of the mode frequency $\omega(T)$ and and the linewidth $\Gamma(T)$ are given by

$$\omega(T) = \omega(0) - A[(\exp(h\omega/kT) - 1)^{-1} + 1/2)], \tag{1}$$

and

$$\Gamma(T) = \Gamma(0)[(\exp(h\omega/kT) - 1)^{-1} + 1/2)]. \tag{2}$$

A fit to the cubic anharmonicity model is shown by the continuous line in figure 7b, and is seen to provide a satisfactory account of the temperature variation of the Raman mode. The

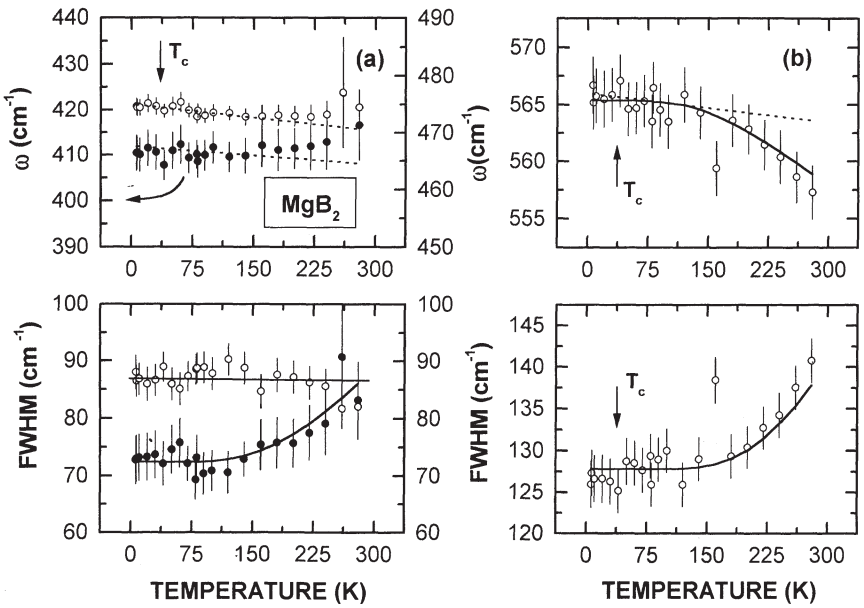

Figure 7. **(a)** Temperature dependence of the frequency and width of the infrared modes at 410 cm^{-1} (filled circles) and 475 cm^{-1} (open circles). The dotted lines are fits corresponding to quasi-harmonic contribution and the continuous lines are guides for the eye. **(b)** Temperature dependence of the frequency and width of the mode at 560 cm^{-1}. The dotted lines are fits corresponding to quasi-harmonic contribution and the continuous lines are calculated based on cubic anharmonicity model.

dashed lines represent the quasiharmonic contribution, that has been estimated (Sood *et al* 1981) from the known value of the thermal expansion coefficient (Jorgensen *et al* 2001) and the mode Gruneissen parameter (Goncharev *et al* 2001), and is clearly inadequate to account for the variation of mode frequency with temperature. The importance of anharmonic effects to account for the temperature dependence of in the Raman mode is in consonance with the theoretical calculations (Bud'ko *et al* 2001). Martinho *et al* have followed the temperature dependence of the Raman mode and have observed a large variation of width that has been attributed to anharmonicity. However, no change in the mode frequency is seen in their experiments.

We also note from figure 7 that no change in either the mode frequency or width is observed below the superconducting transition. It is known (Zeyher & Zwicknagel 1990) that in general, the opening of the gap below T_c, has a small effect on the phonon frequency, $\sim 2\Delta / W$, where 2Δ is the superconducting gap and W is the band width. Further, while phonons less than the gap energy are expected to soften, those above the gap energy, as in the present case, are expected to harden. In fact, theoretical calculations based on strong coupling theory predict (Liu *et al* 2001) a hardening of $\sim 12\%$ across T_c. However, we observe no such changes across T_c in the present experiments, as also the case in the experiments of Martinho *et al* and Tu *et al*.

4.2 *Electron-phonon interaction*

It is well known that electron–phonon interaction results in a softening of the mode frequency and an increase in the linewidth. From the measured linewidth, the electron–phonon coupling

constant can be estimated using Allen's formula (Allen 1974) which relates the linewidth (Γ_i) for the ith phonon mode to the dimensionless electron–phonon coupling constant λ_i.

$$\Gamma_i = (2\pi/g_i)N(E_F)\lambda_i\omega_{b,i}^2, \tag{3}$$

where $N(E_F)$ is the density of states at the Fermi level per spin and cell, g_i is the mode degeneracy, and $\omega_{b,i}$ is the bare frequency, viz., in the absence of electron–phonon interaction.

We proceed to estimate λ_i for the Raman mode that is supposed to have the largest electron–phonon interaction. In our present experiments, we observe the Raman mode at 560 cm^{-1}, with a width of 140 cm^{-1}. Using these and $N(E_F) = 0{\cdot}37$ states/eV/fu/spin (An & Pickett 2001; Kong *et al* 2001) leads to $\lambda_i = 3{\cdot}1$, a value considerably larger than the accepted value of $\sim 0{\cdot}7$. This discrepancy arises because we have used the measured frequency in place of bare frequency, and the measured line width can have additional contributions from disorder and anharmonicity. However, the disorder contribution to the Raman linewidth, is probably small, as Raman experiments on single crystals (Hlinka *et al* 2001) yield linewidth similar to those in polycrystalline pellets. To take care of anharmonicity effects, we use the measured linewidth at low temperature, viz., 125 cm^{-1}. As for the bare frequency, $\omega_{b,i}$, we use the Raman mode frequency (984 cm^{-1}) in AlB_2 – a system in which the electron–phonon interaction is not significant (Bohnen & Renker 2001). This results in a reasonable value of $\lambda_i = 0{\cdot}99$. The enormous softening of the Raman mode from a value of 984 cm^{-1} in AlB_2 (Bohnen & Renker 2001) to 560 cm^{-1} in MgB_2, a consequence of the strong electron–phonon interaction in MgB_2, calls for further systematic experiments to probe the variation of this mode with Al doping.

We dedicate this article to Dr T S Radhakrishnan, on his 60th birthday, for his long standing contributions to the research and development in superconductivity at the Materials Science Division, IGCAR. The authors also thank M Premila, T N Sairam, S Kalavathi, G L N Reddy, and V S Sastry for their collaboration in the present work.

References*

Allen P B 1974 *Solid State Commun.* 14: 937
An J M, Pickett W E 2001 *Phys. Rev. Lett.* 87: 4366
Bohnen K P, Renker B 2001 *Phys. Rev. Lett.* 87: 5771
Bordet P, Mezonar M, Nunez-Regueiro M D, Rogado N, Regan K A, Hayward M A, He T, Loureiro S M, Cava R J cond-mat/0106585
Bud'ko S L, Lapertot G, Petrovic C, Cunningham C E, Anderson N, Canfield P C 2001 *Phys. Rev. Lett.* 86: 1877
Buzea T, Yamashita T 2002 *Superconductor Science and Technology* (in press)
Canfield P C, Finnemore D K, Budko S L, Ostenson J E, Lapertot G, Cunningham C E, Petrovic C 2001 *Phys. Rev. Lett.* 86: 2423
Chen X K, Konstantinovic M J, Irwin J C, Lawrie D D, Franck J P 2001 *Phys. Rev. Lett.*, 87: 157002
Goncharev A F, Strzhkin V I, Gregoryanz E, Hu J, Hemley R J, Mao H K, Lepertot G, Budko S L, Canfield P C 2001 *Phys. Rev.* B: 1, September

*References in this list are not in journal format

Hlinka J, Gregora I, Pokorny J, Plecenick A, Kus P, Satrapinsky L, Benacka S 2001 *Phys. Rev.* B64: 140503 (R)
Jemima Balaselvi S, Bharathi A, Reddy G L N, Sastry V S, Hariharan Y, Radhakrishnan T S 2001 *Proc. DAE Solid State Physics Symp. Bombay* - (in press).
Jemima Balaselvi S, Bharathi A, Reddy G L N, Sastry V S, Hariharan Y, Radhakrishnan T S 2002 *Physica C* - (communicated)
Jorgensen J D, Hinks D G, Short S 2002 *Phys. Rev.* B64: 224522
Kalavathi S, Bharathi A, Jemima Balaselvi S, Reddy G L N, Sastry V S, Hariharan Y, Radhakrishnan T S 2001 *Proc. DAE Solid State Physics Symposium*, Bombay (in press)
Kang W N, Kim H J, Choi E M, Jung C U, Lee S 2001 *Science* 292: 1521
Kong Y, Dolgov O V, Jepsen O, Andersen O K 2001 *Phys. Rev.* B64: 0202501 (R)
Khazakov S M, Angst M, Karpinski J cond-mat/0103350
Kortus J, Mazin I I, Balaschenko K D, Antropov V P, Boyer L L 2001 *Phys. Rev. Lett.* 87: 4656
Liu A Y, Mazin I I, Kortus J 2001 *Phys. Rev. Lett.* 87: 087005
Lorenz B, Meng R L, Chu C W 2001 *Phys. Rev.* B64: 12507
Martinho H, Martin A A, Rettori C, de Lima O F, Ribero R A, Avila M A, Pagiluso P G, Moreno N O, Sarrao J L cond-mat/0105204
Mehl J, Papaconstantopoulos D A, Singh D J cond-mat/0104548
Moritomo Y, Xu S cond-mat/0104568
Nagamutsu J, Nagakawa N, Muranaka T, Zenitani Y, Akimitsu J 2001 *Nature (London)* 410: 63
Osborne R, Goremychkin E A, Kolesnikov A I, Hinks D G 2001 *Phys. Rev. Lett.* 87: 17005
Paranthaman M, Thompson J R, Christen D K 2001 *Physica C* 355: 5
Sood A K, Arora A K, Umadevi V, Venkataraman G 1981 *Pramana* 16: 1
Slusky J, *et al* 2001 *Nature (London)* 410: 343
Sundar C S, Premila M, Sairam T N 2001 *Proc. DAE Solid State Physics Symposium*, Bombay (in press)
Takenobu T, Ito T, Chi D H, Prassides K, Iwasa Y cond-mat/0103241
Tu J J, Carr G L, Perebeinos V, Homes C C, Strongin M, Allen P B, Kang W N, Choi E M, Kim H J, Lee S K cond-Mat./0107349
Yildrim T 2001 *Phys. Rev. Lett.* 87: 370001
Zeyher R, Zwicknagel G 1990 *Z. Phys.* B78: 175